Surface structure and segregation of bimetallic bcc-type alloys

1999 J. Phys.: Condens. Matter 11 8377

(http://iopscience.iop.org/0953-8984/11/43/302)

J. Phys.: Condens. Matter **11** (1999) 8377–8396. Printed in the UK PII: S0953-8984(99)02626-0

Surface structure and segregation of bimetallic bcc-type alloys

K Heinz† and L Hammer

Universität Erlangen–Nürnberg, Lehrstuhl für Festkörperphysik, Staudtstrasse 7, D-91058 Erlangen, Germany

E-mail: kheinz@fkp.physik.uni-erlangen.de

Received 16 March 1999

Abstract. We report on the surface structure and segregation of bimetallic bcc-type alloys, on which so far there has been comparably little emphasis in the literature—unlike the case for fcc-type material. The focus is both on ordered and on substitutionally disordered alloys: it is shown that for a given slab of the surface, ideal chemical order or disorder, respectively, are rather limiting cases. For chemically ordered samples, surface segregation can lead to both some disorder and new ordered phases. In the case of substitutionally disordered alloys, segregation leads to a layer-dependent compositional profile. Depending on the openness of the surface, as is evident from the investigation of different low-index surfaces, this profile may extend deep into the surface. Correspondingly, the geometrical multilayer relaxation is unusually deeply extended, too, as comparison to the related pure-metal surfaces shows. Clearly, there is a correlation between geometrical relaxation and chemical segregation: though the relaxation of the first few layer spacings can be lifted by, for example, hydrogen adsorption, it is stabilized in deeper layers by the frozen-in segregation profile. On the other hand, surface segregation is modified by adsorbates strongly bonding to one of the constituents.

1. Structure and stoichiometry of alloy surfaces' deviations from bulk termination

It is well known that upon creation of a surface of an elemental crystal, a substantial degree of atomic reordering can take place within a certain atomic slab of the surface. As a rule, more or less strong relaxations of the first few layer spacings (*multilayer relaxation*) are observed that still preserve the lateral symmetry given by the bulk, but frequently also symmetry-breaking (and often bond-breaking) movements of atoms take place (*surface reconstruction*). Of course, this scenario holds also for compound material, in particular alloy surfaces. Yet, the situation becomes even more diverse and sometimes rather complex because of the increased size of the surface unit cell and the additional chemical degrees of freedom. In order to introduce some systematics, it is useful to differentiate between chemically *ordered* and *disordered alloys* [1,2]. Chemical order (disorder) is likely to develop if the enthalpy of mixing is negative (near zero), whilst a significant positive value leads to the phase separation of the constituents. In ordered alloys the different chemical species exclusively occupy sublattices of the crystal lattice. Frequently, such a chemically ordered material is also called an *intermetallic compound* (denoted by A_nB_m with n, m integer), though in some of the literature this term is only used if the compound lattice spanned by all atomic positions is different from the constituents' lattices (an example is NiAl which is of CsCl structure with atoms residing at bcc-type sites, whilst both Ni and Al have fcc lattices).

† Author to whom any correspondence should be addressed.

0953-8984/99/438377+20$30.00

In the first place, as regards the above-mentioned additional chemical degrees of freedom, the surface of an ordered alloy can 'choose' at which layer it terminates when, according to the given surface orientation, different surface-parallel layers are of different chemical composition. Moreover, due to the broken symmetry of bonding at the surface there may be some *rippling* (or *buckling*) of surface layers, i.e. the positions of the different atoms in the layer unit cell must not fall within the same plane (as applying to bulk layers). Additionally and more importantly, however, some chemical reordering can take place in the surface, as some of the atomic neighbours formerly present in the bulk are now missing. This chemical reconstruction can occur in parallel with a geometrical reordering, and some observations indicate that the two processes are coupled. When the chemical reordering is not stoichiometry preserving it is called *segregation*, whereby this term is used both for the ordering process itself and the stoichiometric final state of the surface. As regards the latter, segregation strictly speaking denotes an *enrichment* of a certain species in the surface (rather than its *depletion*), but frequently it is used also more generally for any deviation from bulk stoichiometry, as depletion of one species means enrichment of the other. Usually, the species with the smaller homogeneous bonding enthalpy is observed to segregate to the surface, so minimizing the surface tension. Segregation processes in ordered alloys can lead to new ordered phases in the surface slab different from the bulk structure, but—as we will see—also to some chemical disorder with sublattices not exclusively occupied by a single species (*anti-site occupation*). This applies in particular to the case where disorder has been induced during the cleaning procedure of a surface, e.g. by sputtering, and the subsequent annealing process does not restore the (possibly new) order completely.

This bridges to the many examples of disordered alloys (also called *solid solutions*). There can be *interstitial disorder* with one of the species occupying interstitial sites, but the large majority of investigations address *substitutionally disordered alloys* (also called *random alloys*). Here all atoms reside at lattice sites, yet without any chemical preference (for binary alloys, frequently the notation A_xB_{1-x} is used, with $x < 1$ denoting the bulk concentration of species A). For random alloys the termination of the surface is not an issue, as all bulk layers exhibit the same stoichiometry. Yet, due to segregation processes, different layers in the surface slab can eventually exhibit different stoichiometries, i.e. a certain *segregation profile* forms characterized by the concentrations x_i of species A in the ith layer. With increasing depth, x_i converges to the bulk value ($x_i \approx x$ for $i \gg 1$). Of course, the segregation profile corresponds to some degree of (newly established) order, i.e. segregation can both destroy and restore chemical order. In fact, chemical order–disorder transitions observed in bulk alloys have been seen to be shifted to higher temperatures in the surface, so influencing the critical phenomena heavily (see, e.g., references [3,4]). In parallel to segregation, of course, multilayer relaxations take place, with interlayer spacings $d_{i,i+1}$ between the ith and $(i + 1)$th layers deviating from the bulk value d_0, and some coupling between x_i and $d_{i,i+1}$ must be expected. As in the case of ordered alloys, the different bonding situation within the surface, compared to that within the bulk, can induce some (layer-dependent) rippling of layers.

The above-described rich scenario of what can happen geometrically and/or chemically at an alloy's surface—though it already modifies its physical and chemical properties considerably [5]—is not yet complete. First, one should note that all features mentioned must be expected to depend on the crystallographic orientation of the surface. Also, we have to expect that adsorption of atoms of a third species on the alloy's surface can modify not only the surface structure (as is well known for elemental solids) but also the layer-dependent equilibrium composition, e.g. when the adatoms 'prefer' bonding to one of the constituents and the temperature allows for the necessary diffusion processes. Of course, this considerably affects the chemical properties of the compound. Last but not least, segregation and reordering

are not bound to happen just at the surface, i.e. the solid's interface with the vacuum, but should also take place (in modified form) at inner interfaces, so influencing e.g. the mechanical properties of the alloy.

In the present paper we give examples of almost all features of the structural–compositional reordering described above. We concentrate here on the clean surfaces of both random alloys of bcc structure and ordered alloys of CsCl (or B2) structure. The latter are sometimes also called bcc type, as the atoms (regardless of their chemical nature) occupy a bcc lattice. In comparison to the case for fcc-type alloys, which are more frequently addressed in the literature, the atomic packing is less dense, i.e. the atoms have fewer nearest neighbours, so pronounced layer relaxations can develop, as is again well known for elemental bcc crystals. As only a few groups have performed structure–stoichiometry-related work on this subclass of binary alloys (except as regards investigations for NiAl and a few other alloys to be cited below), we can concentrate on the recent work of our own group dealing with different surfaces of the ordered alloys FeAl and CoAl and the random compound Mo_xRe_{1-x}. Our results mainly stem from investigations by means of quantitative low-energy electron diffraction (LEED). In contrast to its power for determining the precise surface geometry, the chemical resolution of the method is not well known. The latter arises from the different chemical constituents' scattering characteristics (phase shifts) if these are sufficiently different. This gives access to the surface stoichiometry and the type of chemical order, when this is present. So, the LEED analysis provides the layer-dependent geometry and stoichiometry in one step (for an up-to-date review of the method, see reference [6]). In addition, Auger electron spectroscopy (AES) was applied, supplying independent information on the surface composition—averaged, however, over the escape depth of the Auger electrons.

Before addressing the examples below, the reader should realize that prior to the investigation of a surface, its cleaning, e.g. by sputtering, usually causes considerable surface destruction, both geometrically and chemically. For elemental metals, thermal annealing restores the geometrical order in most cases with ease, as surface atoms need to diffuse only over small distances. In the case of compound surfaces, however, usually additional chemical disorder is created, in particular by preferential sputtering of one of the constituents. Then the restoration of the former stoichiometry or chemical order can involve long-range diffusion processes, e.g. from the deep-lying bulk. Consequently, though being geometrically already rather well ordered, a certain surface slab—as the temperature is varied, and controlled by the energies and entropy involved—can pass through a number of chemically intermediate (metastable) states on its way to the eventual stable chemical structure. Sometimes it may be hard to decide whether a certain stoichiometric state or chemical order reached is stable or still metastable and only frozen in, in particular when high activation energies are involved. Some further complication can arise on annealing at high temperatures, when one of the constituents evaporates preferentially.

2. CsCl-type ordered alloys: bulk termination and surface reordering

As described above, the equilibrium state of an alloy surface can but must not correspond to the state resulting from bulk truncation. The actual behaviour depends on both the material and the crystallographic face, as demonstrated in the following subsections. For the reader's convenience, some different surface orientations of a CsCl-type alloy AB are illustrated in figure 1. We recall for the (100), (111) and (210) orientations that surface-parallel layers consist of either A or B atoms, and consequently two surface terminations are possible. In contrast, the (110) and (310) surfaces have layers of mixed stoichiometry. We should emphasize, however, that for higher-index surfaces the discrimination between the two cases becomes more and

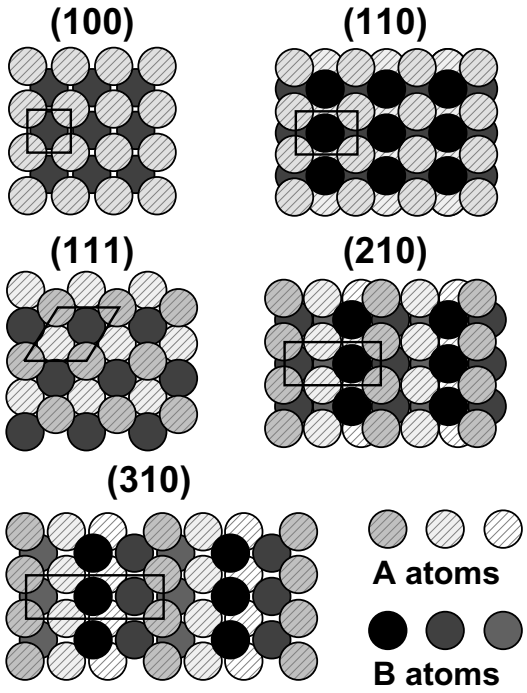

Figure 1. Atomic hard-sphere surface models of different faces of bulk-terminated CsCl-type alloy. The (100), (111) and (210) surfaces consist either of A or B atoms, where here A atoms (hatched) are chosen to terminate the surface. The other surfaces consist of mixed layers. The shading of the atoms decreases with increasing depth of their location. The surface unit cell is marked in each case.

more meaningless when layer distances become smaller and smaller with increasing openness of the surface.

2.1. Bulk-terminated or nearly bulk-terminated composition

In earlier reviews, surfaces of ordered alloys have frequently been reported to be chemically bulk terminated [1, 2]. This holds in particular for the NiAl system, which has so far been the most widely investigated alloy. For NiAl(110), for which the surface termination is not an issue, because all layers exhibit the same mixed stoichiometry, an ordered rippling of the top layer with Al atoms pulled out of the surface by $r_1 = 0.20$ Å relative to Ni atoms has been reported from both experimental work [7–10] and first-principles calculations [11–13]. The corresponding ordered rippling in the second layer is already very small ($r_2 = 0.02$ Å) and only some weak relaxations of interlayer spacings (relative to the centre-of-mass planes) have been found [9]. The reader should note that the rippling is still in accordance with a 1×1 structure due to the layer unit mesh containing two atoms. Table 1 shows that similar features have also been found for CoAl(110) [14] and FeRh(110) [15]. However, it is important to emphasize that both for NiAl and for FeRh ideal chemical order according to bulk truncation has been assumed in the LEED analyses [9, 15], though for FeRh non-stoichiometric islands exhibiting a 3×1 reconstruction were also observed [15]. Indeed, allowing for chemical disorder in the LEED analysis of CoAl(110), as much as 20% of the Al atoms of a single layer were found to be substituted for with Co. Up to now there is no explanation for that disorder, in particular in view of the comparably large heat of formation (54 kJ mol^{-1} [16]) as well as in view of the disorder being restricted to the second layer only. Moreover, the substitutional Co atoms do not reside exactly at the former Al positions but—as established by a special version of TensorLEED [14]—are displaced outward by $\Delta = 0.05$ Å, causing a disordered rippling of the second layer as demonstrated in figure 2. For NiAl the ordered rippling has been traced

Table 1. Geometrical and chemical structure of three bcc(110) binary alloys as determined by quantitative LEED (dashes indicate that the respective parameters have not been varied in the course of the analysis).

		NiAl(110) (reference [9])	FeRh(110) (reference [15])	CoAl(110) (reference [14])
Bulk layer spacing	d_0 (Å)	2.04	2.11	2.02
Interlayer relaxations	$\Delta d_{12}/d_0$ (%)	−1	+ 1	+ 1
	$\Delta d_{23}/d_0$ (%)	+ 1	0	−1
Ordered rippling	r_1 (Å)	0.20	0.15	0.18
(Al or Fe pulled out)	r_2 (Å)	0.02	—	0.01
Chemical order	1st layer	—	—	Fully ordered
	2nd layer	—	—	20% Al substituted for with Co
Geometrical order	1st layer	—	—	Fully ordered
	2nd layer	—	—	Disordered rippling (Co above former Al site by $\Delta = 0.05$Å)

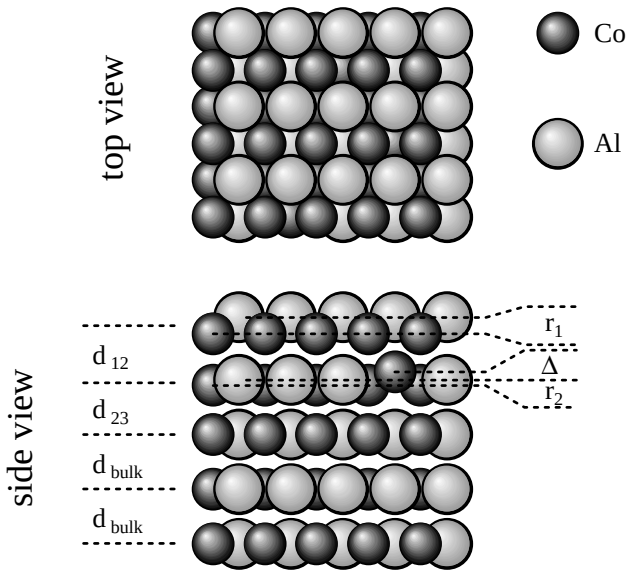

Figure 2. The atomic model for the CoAl(110) surface exhibiting ordered rippling in the top layer and both stoichiometric disorder and disordered rippling in the second layer (after reference [14]). The numerical values of the parameters are given in table 1.

back to the strong localization of the transition metal d electrons [11–13] causing Ni and Al to move in opposite directions. A similar quantitative explanation of the additional disordered rippling of CoAl(110) is still lacking.

In contrast to the (110) orientation of an AB alloy of CsCl structure, the bulk-truncated (100) surface is made up of layers of alternating pure A or B composition. So, only the

termination and the degree of some possible layer relaxations seem to be open questions. In fact, both for NiAl(100) and FeAl(100) the well annealed surfaces exhibit 1×1 diffraction patterns. Quantitative LEED analyses assuming ideal bulk stoichiometry found that the surfaces are exclusively terminated by Al with strong interlayer relaxations, as usual for bcc(100), namely $\Delta d_{12}/d_0 = -8.5\%$, $\Delta d_{23}/d_0 = +4\%$ for NiAl(100) [9, 19] and $\Delta d_{12}/d_0 = -14\%$, $\Delta d_{23}/d_0 = +3\%$ for FeAl(100) [20]. Yet, for NiAl(100), ion scattering experiments indicate some depletion of Al in the top layer [7] or even a nickel termination after rapid quenching from 1400 K to room temperature, in which case, however, by extended annealing, a defect-rich Al-terminated surface could also be prepared [21]. It was speculated that the various surface compositions are due to different timescales holding for surface and bulk diffusion as well as to preferential evaporation [21]. For FeAl(100) a recent reanalysis allowing for deviations from the bulk stoichiometry confirmed both the 100% Al termination and the degree of the layer relaxations found earlier [20], but in addition indicated a 20% Al enrichment in the second layer [22]. In very recent and still unpublished work, we found also for CoAl(111) that the well annealed surface exhibits anti-site occupation in certain layers below the topmost one. This indicates that stoichiometric deviations might be typical rather than due to incomplete annealing. As yet, we cannot judge whether this behaviour is material specific or more general.

2.2. Surface segregation and surface reconstruction

The results at least for FeAl(100) indicate that ordered alloys even at thermal equilibrium need not necessarily exhibit precisely the chemical bulk order at their surface (we recall that in the LEED analyses for NiAl surfaces, bulk stoichiometry had been assumed). This feature is even more pronounced for FeAl(110), for which even no 1×1 phase at all can be prepared [17, 18] and a simultaneous geometrical and chemical restructuring of the surface takes place. This applies also to the (111), (210) and (310) faces of FeAl. We briefly describe the equilibrium states of these surfaces in this subsection. Other reconstructed phases which develop with different annealing temperatures on the way to equilibrium will be addressed in section 2.3. The structural and stoichiometric information available for as many as five different surfaces of FeAl corresponds to an unusually broad data set.

When the sputtered FeAl(110) surface is annealed at about or above 800 °C, an incommensurate superstructure described in matrix notation by

$$\begin{pmatrix} 1 & 0.70 \\ 0 & 1.41 \end{pmatrix}$$

appears in the LEED pattern [17, 18], as also found by x-ray diffraction [23]. Application of quantitative AES shows that the average Al concentration in the surface slab of this phase is enlarged ($c_{\mathrm{Al}} = 0.58$), i.e. Al has segregated to the surface to such an extent that it overcompensates for the original depletion by sputtering [17, 18]. Using an escape depth of 4.2 Å [17], a value that lies between those for Al and Fe, the Al concentration of the top layer of the incommensurate phase is calculated to be $c_{\mathrm{Al}}(1) = 0.67$. This corresponds nearly exactly to the stoichiometry of $FeAl_2$. A surface model with a quasihexagonal arrangement of atoms and with each Fe atom laterally surrounded by six Al atoms as displayed in figure 3 accounts fully both for the superstructure and the stoichiometry observed, and is confirmed by x-ray reflectivity measurements [23].

Whilst segregation of Al taking place in the FeAl(110) surface might seem surprising in view of its nearly close-packed surface-parallel layers, one is inclined to expect it even for the (310), (111) and (210) surfaces as these are increasingly more open. In fact, for all three cases considerable Al segregation has been observed, with the result that the Al concentrations as averaged over the surface slab and determined by AES were c_{Al} = 0.72,

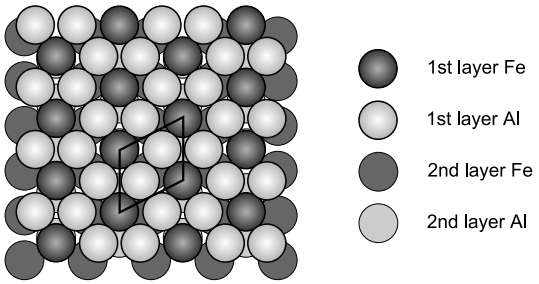

Figure 3. The atomic model for an FeAl(110) surface prepared by annealing at about 600 °C. The top layer exhibits the stoichiometry of $FeAl_2$ and is incommensurate with the bulk-like subsurface layers (after reference [18]).

0.81 and 0.67, respectively [18]. These values already indicate that there is no straightforward correlation between surface openness and degree of segregation. The reason behind this might be related to the significant faceting that the surfaces undergo during annealing in parallel with Al segregation [18]. So, for the (310) face after annealing above 600 °C, facets with preferential (100) orientation and an aluminium excess of two Al extra layers on top of the FeAl bulk are observed. Annealing of the (111) face at above 700 °C leads to three extra Al monolayers on top of the Al-terminated bulk. A 3×3 superstructure is produced which has been interpreted as being (yet is not quantitatively determined to be) due to microfacets forming pyramid-like structures as displayed in figure 4. Similarly, a 3×1 superstructure is observed on the FeAl(210) surface with an extra $\simeq$1.5 Al monolayers on the Al-terminated bulk, consistent with alternating (100) and (110) microfacets as displayed in figure 5 [18]. Interestingly, faceting has also been observed for clean bcc metal surfaces, namely Mo(111)

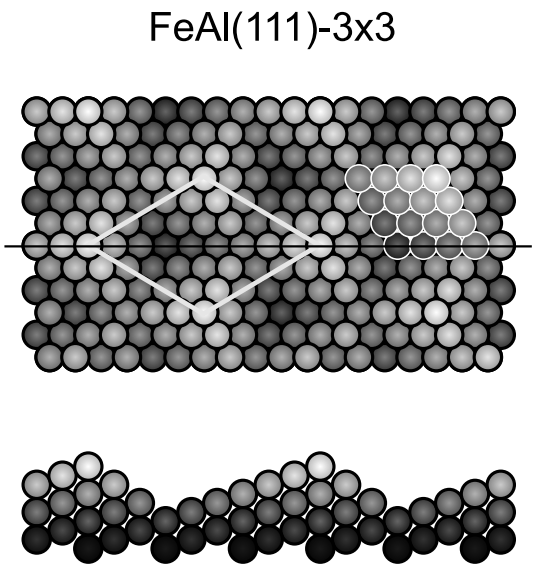

Figure 4. A tentative surface model in on-top and side views for FeAl(111) as prepared by annealing at above 700 °C. Nearly close-packed Al microfacets form pyramid-like units arranged in a 3×3 superstructure (after reference [18]).

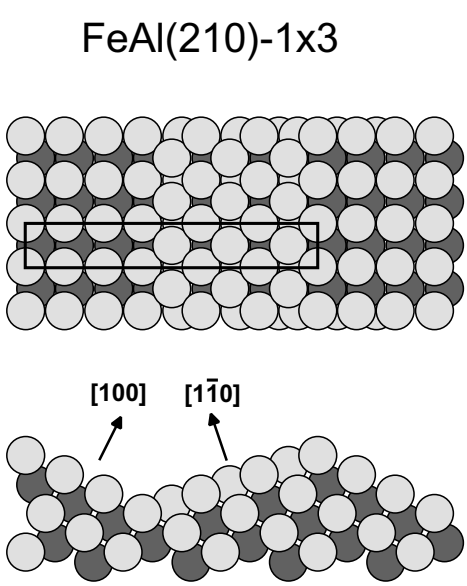

Figure 5. A tentative surface model in on-top and side views for FeAl(210) as prepared by annealing at above 600 °C. Facets of (100) and (110) orientation are arranged to form a 3×1 superstructure (after reference [18]).

and W(111). It is induced by the adsorption of certain other metal atoms, as a consequence of which the surface needs to be fully covered (for a recent review, see reference [25]). This seems to be consistent with the considerable degree of segregation accompanying the faceting in the present case.

To achieve a qualitative understanding of the observed segregation phenomena, it is useful to recall the energy balance for both the binary alloy's bulk and its surface. As mentioned in the introductory section, the heat of formation (free enthalpy of formation ΔH), determined as the difference of the heterogeneous and (averaged) homogeneous bonding energies, dominates the bulk properties, i.e. the ordering of the two constituents into two sublattices. At the surface, bonds of certain atoms are truncated, and this may induce some chemical reordering or segregation of atoms to reach the new minimum of the free enthalpy. In a simple 'broken-bond model' (see, e.g., reference [26]) neglecting entropy contributions and assuming that the lattice geometry remains unchanged, the free enthalpy is reduced when—as a result of the reordering or segregation—only the weakest bonds are broken, i.e. when the element with the weakest homogeneous bonding energy has segregated to the surface (hereby, the corresponding energy gain depends on the difference of the heats of sublimation of the two constituents). As a consequence, surface orientations with elementally pure layers will be terminated by the element with the weakest homogeneous bonds. For surfaces with mixed layers, however, the above energy gain has to be balanced against ΔH, which is the energy that has to be expended when a segregation process creates anti-sites. Consequently, the surface of this alloy will remain bulk terminated if ΔH is sufficiently high. With decreasing ΔH, segregation becomes more and more probable until at rather low values, such as those for random alloys, segregation dominates the chemical properties of the surface (see section 3). Yet, the situation is even more complex: in undergoing a geometric reconstruction, the surface has an additional degree of freedom to minimize its energy, so segregation can take place in spite of the rather large values of ΔH.

For transition metal aluminides, the heat of sublimation is generally 20–30% smaller for Al than for the transition metal [27]. Thus, Al termination is expected whenever possible. Comparing the different ordered bcc-type alloys dominantly considered in the present section,

namely FeAl, CoAl and NiAl, it appears that FeAl with $\Delta H = 25.1$ kJ mol^{-1} [16] has by far the lowest free enthalpy of formation (ΔH(CoAl) $= 54.2$ kJ mol^{-1} [16]; the value for NiAl varies: ΔH(NiAl) $= 58.9$ kJ mol^{-1} [16] or 72 kJ mol^{-1} [31, 32]). Consequently, the driving force for lowering the surface free energy by Al surface segregation is much higher for iron-based aluminides than for those based on nickel and cobalt. The prediction for segregation in layers below the top layer is straightforward only for layers in which some atomic bonds are still broken. This is true for the second and third layer in the (111)-oriented surface, and we do indeed observe strong Al segregation there. As we have seen, even a geometric reconstruction of this surface takes place. This holds also for the (110), (210) and (310) surfaces of FeAl. In any case, in view of the low enthalpy of formation of FeAl, segregation of Al is more favourable for this alloy than for the others, as the energy needed to form anti-sites is lowest. These arguments should hold also for aluminides of other metals near the group VIA of the table of elements (e.g. Cr, Mo, W) which have rather low values of ΔH similar to that of FeAl [33]. So, their segregation properties should be equally pronounced. We emphasize, on the other hand, that even for NiAl and CoAl some anti-site occupation takes place, i.e. ideal bulk termination must be considered as a rather limiting case.

2.3. Frozen-in surface reconstructions of ordered FeAl surfaces

As already mentioned, a surface initially sputtered for cleaning purposes and subsequently annealed to allow for reordering might, on its way to equilibrium, pass through different, rather well defined states of chemical and/or geometrical order. They can be frozen in for investigation and are frequently (meta)stable at room temperature, so technical application might not be ruled out.

The best-investigated face of FeAl in this respect is the (100) surface. Figure 6 displays

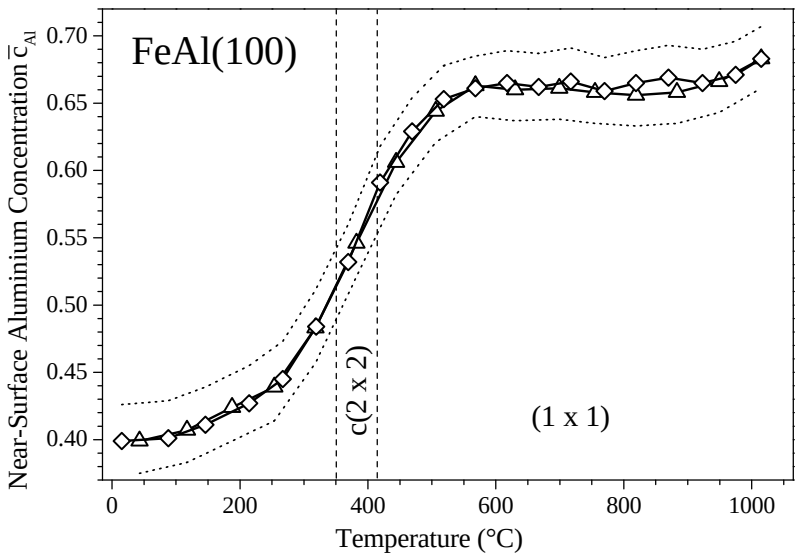

Figure 6. The average Al concentration in the surface slab of FeAl(100) when annealed following initial sputtering for about two minutes at each temperature point given (squares and triangles denote two different, but identically prepared samples). The broken curves mark the error limits for the determination of the concentration by AES due to the uncertain knowledge of the matrix factor (after reference [25]).

the Auger signal measured as a function of the annealing temperature. The latter was held constant for about two minutes at each point given, yet there was no significant change of the stoichiometry when longer annealing times were used. As described above, the 1×1 structure appears only at above about 700 °C. In the small temperature range 350–410 °C, a sharp $c(2 \times 2)$ superstructure is observed. A detailed LEED structure analysis of this phase has shown that it is due to a deeply extending reordering of the surface, resulting in a structure which deviates considerably from the former order of FeAl [22]: a whole slab of $Fe_3Al(100)$ layers has developed, forming the $c(2 \times 2)$ superstructure with respect to the FeAl substrate on which it must reside. Only six such layers could be identified safely by LEED, due to the finite penetration depth of electrons, but the Fe_3Al slab is most probably even thicker. Figure 7 displays the structure schematically; the structural parameters are given in the figure caption. Except for the capping full Al layer, only small deviations from the ideal Fe_3Al stoichiometry are detected [22]. As the lattice parameter of Fe_3Al differs by only 0.5% from that of FeAl, obviously a rather unperturbed reordering-like growth of the $D0_3$-type Fe_3Al takes place. In fact, inspection of the Fe–Al phase diagram tells us that the concentration-versus-temperature

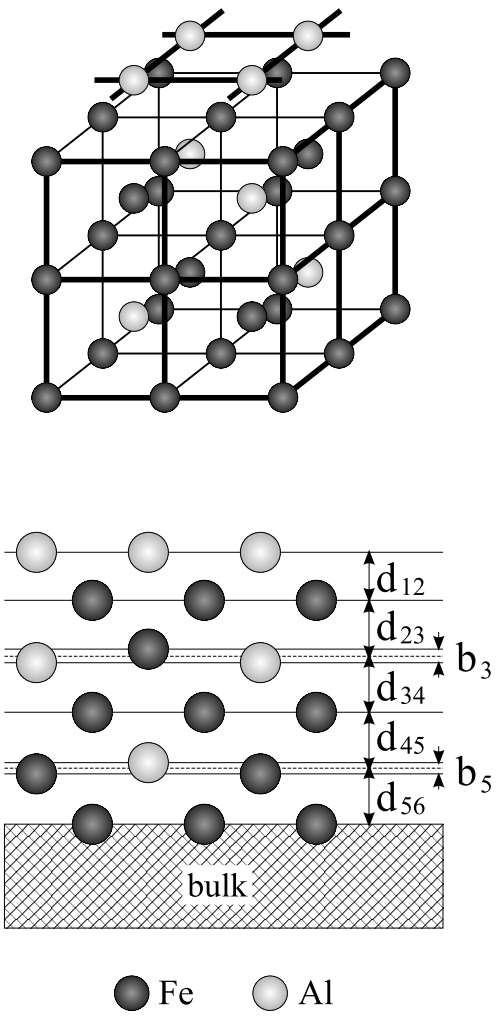

Figure 7. A perspective view of the Al-covered Fe_3Al interface (top) residing on the FeAl(100) substrate. The parameters given in the side view (bottom) were determined as $d_{12} = 1.255$ Å, $d_{23} = 1.490$ Å, $d_{34} = 1.445$ Å, $d_{45} = d_{56} = 1.447$ Å (=bulk value of Fe_3Al), $b_3 = 0.08$ Å, $b_5 = 0.03$ Å (after reference [22]).

curve given in figure 6 passes right through the area where Fe_3Al is stable [22]. This indicates that the new chemical order develops via temperature-controlled stoichiometric changes in the full surface slab rather than by a gradual layerwise growth. So, with effectively an equilibrium structure at hand, one should expect a surface termination typical for $Fe_3Al(100)$. Indeed, a well annealed $Fe_{70}Al_{30}(100)$ crystal, which still exhibits the $D0_3$ structure in its bulk, shows almost identical LEED intensity spectra [28] which, however, have not been quantitatively analysed yet. The Fe_3Al slab on top of the FeAl(100) bulk exhibits interlayer spacings rather typical for bcc(100) surfaces—e.g. the first interlayer distance (involving the capping Al layer which one may interpret as an Al-enriched mixed layer) is reduced by $\Delta d_{12}/d_b = -13\%$. Probably due to the chemical homogeneity of the top layer, the latter is unbuckled, whilst mixed layers exhibit some small degree of buckling (b_3, b_5) decaying quickly with layer depth.

We should mention that the NiAl(100) surface, which is isostructural to FeAl(100), also exhibits a superstructure when annealed between 500 and 700 °C after sputtering, though this is of rather different symmetry, namely NiAl(100)–c($\sqrt{2} \times 3\sqrt{2}$)R45° [7, 29]. Low-energy ion scattering experiments have shown [7, 21] that only two-thirds of the top layer consists of Al atoms; the rest are either Ni atoms [7] or vacancies [21]. The atoms in the top layer are arranged to produce the c($\sqrt{2} \times 3\sqrt{2}$)R45° superstructure observed; the layers below are bulk-like [7, 21, 29]. However, it was also reported that the superstructure is due to some surface contamination [30].

Even after annealing the FeAl(100)–c(2×2) phase for an extended period at 400 °C, the superstructure remains. This holds also for metastable states of the other faces investigated for FeAl. Qualitatively, the development of the surface stoichiometry with annealing temperature for the (110), (111), (210) and (310) faces is similar to that for the (100) face given in figure 6 [18]. For the (110) face a 2×1 superstructure develops in exactly the same temperature range as the c(2×2) structure of the (100) orientation (around 400 °C), indicative that again a Fe_3Si slab may have formed below the surface. Indeed, the arrangement of $Fe_3Al(110)$ on FeAl(110) produces a 2×1 superstructure as observed, and a preliminary quantitative LEED analysis [18] again identifies a thick Fe_3Al slab which must reside on the FeAl(110) substrate (a missing-row model proposed earlier [17] can be ruled out). With further increasing annealing temperature, the surface layers gradually transform to the bulk-like 1:1 stoichiometry except for the top layer which, as described in section 2.1, ends up enriched in Al, i.e. as a $FeAl_2$ layer incommensurate with the layers below.

Quantitative structure analyses become more and more demanding with increasing openness of a surface. So, for the (111), (210) and (310) surfaces of FeAl, no quantitative structural data are available. The (111) face exhibits an intermediate ($\sqrt{3} \times \sqrt{3}$)R30° superstructure which is best developed at 480 °C, corresponding to an average Al concentration $c_{\mathrm{Al}} = 0.69$. As the (111) surfaces of Fe_3Al and FeAl have the same lateral unit mesh, the superstructure must be due to extra surface atoms residing on either surface slab. For both cases, reasonable Al-adatom models have been proposed [18].

3. Random bcc-type alloys: layer-dependent relaxation and segregation

In the above sections we have seen that the bulk termination of a certain ordered alloy is only a limiting case for its surface. Segregation takes place—more or less pronounced—also in ordered alloys, and even considerable chemical–geometrical reconstructions can be observed. The other limiting case is bulk termination as the surface of a random alloy. The random elemental distribution typical for the bulk must not hold for layers in the surface, and some ordering may take place, possibly coupled to the simultaneous relaxation of layer spacings. In the following, corresponding data are presented for the random alloy Mo_xRe_{1-x}

for different values of the bulk concentration x ($x = 0.95, 0.85, 0.75$) as well as for different surface orientations, i.e. (100), (110) and (111). As degrees of layer relaxation can be rather high in bcc-type metals, our focus on bcc-type alloys provides an increased chance of detecting possible correlations between segregation and relaxation. Also, with Mo and Re having almost the same atomic size, both relaxation and segregation are practically free from strain effects, i.e. only controlled by the energetics of bonding. Additionally, we provide data for Mo_xRe_{1-x} surfaces covered by full layers of hydrogen (saturation coverage). Whilst for this case the segregation profile remains built in, the multilayer relaxation due to surface-truncation effects is largely lifted, so providing further insight into the possible coupling between segregation and relaxation. In addition, structure determinations for the different faces of pure molybdenum, both clean and hydrogen covered, are available for comparison to the case for the alloy. We complement this rich data set with investigations of carbon and oxygen adsorption on the alloy surface influencing both the surface structure and the stoichiometry.

3.1. Oscillatory layer-dependent segregation and relaxation

To start with, we concentrate on the layer-dependent segregation and relaxation of $Mo_xRe_{1-x}(100)$ for $x = 0.75$ (we remind the reader that the surface reconstruction typical for Mo(100) [34] is lifted for at least $x \leqslant 0.95$ as confirmed by the excellent agreements between the measured electron diffraction intensities and those calculated for unreconstructed surfaces [35–37]). Table 2, middle column, displays the corresponding data as obtained by quantitative LEED [37] and compares it to relaxational data for pure Mo(100) (the latter were calculated for a hypothetical, unreconstructed surface [38]). In order to give an idea of the accuracy of the parameters, error limits as determined through the variance of the applied

Table 2. Multilayer relaxation and segregation of the (110), (100) and (111) surfaces of $Mo_{75}Re_{25}$ and of pure Mo for comparison (dashes indicate that the respective parameters have not been varied in the course of the analyses).

	(111) ($d_0 = 0.90$ Å)		(100) ($d_0 = 1.56$ Å)		(110) ($d_0 = 2.21$ Å)	
	$Mo_{75}Re_{0.25}$ [44]	Mo [46]	$Mo_{75}Re_{25}$ [37]	Mo* [38]	$Mo_{75}Re_{25}$ [44]	Mo [45]
$\Delta d_{12}/d_0$ (%)	−19.1 (±1.7)	−18.8	−11.9 (±0.6)	−10.7	−2.3 (±0.5)	−4.0
$\Delta d_{23}/d_0$ (%)	−19.1	−18.9	+ 5.1 (±0.6)	+ 2.7	+ 0.4 (±0.5)	+ 0.2
$\Delta d_{34}/d_0$ (%)	+ 15.2	+ 6.4	−3.7 (±0.9)	+ 0.3	0.0 (±1.0)	0.0
$\Delta d_{45}/d_0$ (%)	−4.7	+ 2.2	+ 3.9 (±0.8)	—	—	—
$\Delta d_{56}/d_0$ (%)	+ 0.0	+ 2.1	−2.5 (±1.1)	—	—	—
$\Delta d_{67}/d_0$ (%)	+ 4.1	+ 0.9	+ 1.1 (±1.3)	—	—	—
$\Delta d_{78}/d_0$ (%)	−3.6	0.0	—	—	—	—
$\Delta d_{89}/d_0$ (%)	+ 3.0	−1.6	—	—	—	—
c_1^{Mo} (%)	93 (±15)		99 (±13)		70 (±16)	
c_2^{Mo} (%)	25 (±15)		51 (±14)		79 (±10)	
c_3^{Mo} (%)	77 (±18)		84 (±13)		78 (±9)	
c_4^{Mo} (%)	70 (±20)		72 (±15)		—	
c_5^{Mo} (%)	80 (±20)		—		—	
c_6^{Mo} (%)	72 (±20)		—		—	

* Calculated.

Pendry R-factor [39] are also included in the table. The analysis is sensitive to layer spacings and stoichiometries down to the sixth and fourth layers, respectively.

Evidently, well beyond the limits of error, a strong segregation of Mo to the top layer is detected. In agreement with experiments using LEIS [40] and XPS [41], the best fit results for a top layer consisting practically exclusively of Mo atoms. In contrast, the second layer is considerably depleted in Mo, the third again enriched, and so it is not until the fourth layer is reached that almost bulk-like stoichiometry is seen. So, there is an oscillatory segregational profile similar to that known for many fcc-type alloys [1, 2]. Also, there is an oscillatory relaxational profile, as frequently observed for pure-metal surfaces, too. Yet, the multilayer relaxation of $Mo_{75}Re_{25}(100)$ extends much deeper into the surface than that of pure Mo(100), a result which again is well beyond the limits of error. Whilst the top-layer spacing is contracted by almost the same amount for both surfaces (the contraction is considerable, as is typical for bcc(100) metals), the deviations from the bulk value for deeper spacings are significantly larger for the alloy and extend down to at least the fifth spacing. In contrast, the third spacing of the pure metal is already nearly bulk-like.

Investigation of $Mo_xRe_{1-x}(100)$ for $x = 0.85$ indicates again both an oscillatory relaxation and an oscillatory segregation profile. Yet, whilst the top layer is still exclusively of Mo and its spacing from the second layer still considerably contracted, the oscillatory amplitudes for deeper layers are already slightly reduced compared to the case for which $x = 0.75$. This holds as regards amplitudes of both the segregation and relaxation [37]. The trend towards deeper-layer amplitude reduction seems to proceed with increasing x, though for $x = 0.95$ the error limits for the stoichiometry are too large for safe conclusions to be drawn [37]. So it appears that multilayer segregation influences multilayer relaxation as regards both its magnitude and penetration into the surface. The correlation seems to be the more pronounced, the larger the bulk value of x. We come back to this point in section 3.3.

3.2. Face dependency of the segregation and relaxation

As geometrical multilayer relaxation is well known to depend considerably on the crystallographic orientation, i.e. the openness of a surface [42], it is interesting to investigate whether this holds also for the segregation profile. Table 2 also therefore includes data for the (110) and (111) orientations of $Mo_{75}Re_{25}$ [44] (and of pure Mo [45, 46] for comparison), i.e. for surfaces which, compared to the (100) face, are less and more open, respectively. Indeed, it turns out that the geometrical relaxations for both the alloy and the pure-metal surfaces are the more pronounced the more open the surface. Whilst in the case of the nearly close-packed (110) surface only the top spacing is (slightly) reduced, there are strong relaxations in the (111) surface. In the latter, the first two spacings are both considerably contracted (*double contraction*) which—as applies also to Fe(111) [43]—seems to be typical for bcc(111) metal surfaces. There is no significant surface segregation in the (110) surface and this is, in the light of the above discussion for the (100) face, in agreement with the fact that the relaxations of the alloy and pure-metal (110) surfaces are rather similar. In the case of the (111) surface, the segregation profile seems to be enhanced over that of the (100) surface (we must admit that this is established safely only for the strong Re depletion in the second layer and otherwise may be hidden within the limits of error). Again consistent with the findings for the (100) face, the segregation is accompanied by geometrical relaxations extending considerably deeper into the surface than in the case of the pure metal.

The segregational and relaxational features described above can be qualitatively explained again in the 'broken-bond model' using the homogeneous bonding energies and heats of formation of the elements involved [44]. As already outlined in section 2.2, the element with

the weaker homogeneous chemical bond should segregate to the surface, so minimizing the number of strong bonds broken and so the surface stress. In the light of this, the homogeneous bonding energy of Mo being weaker by 117 kJ mol^{-1} than that for Re is in agreement with the accumulation of Mo in the top layers of the (100) and (111) surfaces. The virtual absence of segregation in the (110) face partially stems from the fact that only two nearest-neighbour (NN) bonds (out of eight bonds) per top-layer atom are truncated by creation of this surface, whilst for atoms in the top (100) and in the top (111) layer the truncation applies to four bonds (in the (111) surface, even atoms in the second and third layer lack NNs, accounting for the increased openness of the surface). Once the top layer is enriched in Mo, the small negative enthalpy of Mo–Re mixing triggers the Re enrichment of the second layer, i.e. an oscillatory segregation profile develops in agreement with observation. This can be interpreted as a trend towards AB ordering (CsCl or B2 structure), and even some critical behaviour in this respect has been reported recently [4].

3.3. Separation of truncation- and segregation-induced multilayer relaxation

The above considerations do not provide any immediate insight into a possible relation between segregation and geometrical relaxation. This can be gained by hydrogen adsorption experiments [49–51], as, with the surface saturated by hydrogen, chemical bonds originally broken by the creation of the surface are largely restored and the former surface relaxation is in many cases lifted to a large extent. This behaviour has been frequently observed with full-coverage hydrogen adsorption on transition metals, at least for not-too-open surfaces for which adatom bonding is only to top-layer atoms (for recent reviews, see references [47, 48]). In principle, this behaviour should be found also for alloy surfaces. With hydrogen made to adsorb at low enough temperatures (e.g. at about 100 K for the present case of $Mo_{75}Re_{25}$), the segregation profile remains frozen in, due to diffusion of alloy atoms being inhibited. So, we expect the relaxation caused by the mere presence of the surface discontinuity to be largely lifted, leaving only the influence of the multilayer segregation. In this sense, H adsorption shows promise as a tool for the separation of truncation- and segregation-induced multilayer relaxation.

Upon hydrogen saturation, the (110), (100) and (111) surfaces of $Mo_{75}Re_{25}$ are covered by rather similar numbers of adatoms (1.4×10^{15}, 1.8×10^{15} and 2.0×10^{15} cm^{-2}, respectively) and exhibit 1×1 LEED patterns corresponding to the phases (110)–(1 × 1)–1H, (100)–(1 × 1)–2H and (111)–(1 × 1)–3H. They have been analysed quantitatively, including the hydrogen adsorption positions [49–51]. The same phases have been observed and analysed for the corresponding orientations of pure Mo; so we find the sole influence of hydrogen adsorption on multilayer relaxation, without it being affected by segregation. Whilst for both H/Mo(110) [45] and H/Mo(100) [52] nearly bulk termination of the substrate is reported, the situation for H/Mo(111) is more complex. This is not only due to the fact that in contrast to the other faces the clean surface shows a pronounced double contraction, but also to the fact that the three adatoms in the surface unit cell undergo bonding to atoms of not only the top substrate layer but also the following two layers. As a consequence, it turns out that the considerable contraction of the top-layer spacing is preserved upon hydrogen adsorption, whilst the contraction of the second spacing is practically lifted and also deeper spacings relax back to almost the bulk value. This was established both by LEED analysis and density functional theory [46].

As expected, the LEED analyses of the hydrogen-saturated $Mo_{75}Re_{25}$(110), (100) and (111) surfaces within the limits of errors produce the same segregation profiles as for the respective uncovered surfaces, i.e. the layer-dependent stoichiometry is indeed frozen in. Using bar plots, figure 8 compares in the panels on the left-hand side the layer relaxations for the

three hydrogen-covered surfaces with the relaxations applying to the clean surfaces [49–51]. On the right-hand side the panels display the relaxation differences from the respective phases of the corresponding pure-Mo surfaces. For the nearly close-packed (110) face, the small contraction of the top-layer spacing is even further reduced, corresponding now to an almost ideally bulk-like-terminated surface, both chemically and geometrically. The differences from the relaxations of clean and H-covered Mo(110) are very small (below 2%). As regards the (100) face, on which hydrogen bonds are still exclusively to top-layer atoms, as bridge sites are occupied [50], the contraction (expansion) of the first- (second-) layer spacing is almost completely lifted, again in nearly quantitative agreement with the behaviour of the related pure-metal face. Yet, the still-considerable relaxations of deeper spacings are almost unchanged. This strongly indicates that the influence of hydrogen does not extend below the second-layer spacing (as could reasonably be expected). Of course, this holds in an equivalent way also for the influence of bond truncation in the case of the uncovered surface. The bonding of hydrogen to exclusively top-layer atoms influences the bonding of the latter to second-layer atoms, which in turn affects their bonding to the third layer, by which the electronic influence of hydrogen seems to be screened. As a consequence and as is also evident from figure 8, the relaxations of spacings below the third layer remain unchanged; their deviations from the bulk spacing are apparently stabilized by the frozen-in segregation profile.

Due to the considerable openness of the (111) surface, its hydrogen-induced behaviour is not that clear cut [49, 51]. The first-layer spacing becomes even more contracted and the second-layer spacing less contracted, though the latter is not fully relaxed (the sum of the two distances is almost unchanged). The expansion (contraction) of the third-layer (fourth-layer) spacing is reversed to a contraction (expansion) and the formerly unrelaxed fifth-layer spacing becomes contracted. Only spacings below the sixth layer remain nearly the same as for the uncovered surface, seemingly again stabilized by the frozen-in segregation profile. This complex relaxation behaviour upon hydrogen adsorption is in agreement with the findings for the pure-Mo(111) face: as hydrogen bonding is to both first- and second-layer atoms [49, 51] and as these have near neighbours in the fourth and fifth layer, respectively, only spacings below are likely to be unaffected by hydrogen adsorption. So, in this region, non-zero relaxations must be stabilized by segregation (cf. figure 8, upper panel). Yet, we should point out that the atomic interactions in an open surface are rather complex, so in the absence of first-principles calculations for disordered alloys, the above considerations must at present be considered rather preliminary, if not in fact speculative.

3.4. Adsorbate-induced segregation

Certainly, the preferential bonding of adsorbates to one of the constituents of the alloy should modify the surface segregation if the experimental conditions allow for the necessary diffusion processes. This was not the case in the above-described case of hydrogen adsorption; for sufficiently increased temperatures, the adatoms would have desorbed. Yet, with strongly bonding adatoms, adsorbate-induced segregation should be observable. For the $Mo_xRe_{1-x}(100)$ surface this was indeed realized, with carbon and oxygen as adatoms on $Mo_{75}Re_{25}(100)$ [49, 53–55].

Carbon atoms on $Mo_{75}Re_{25}(100)$ were observed to develop several ordered phases largely independently of whether the adatoms were brought to the surface by decomposition of adsorbed acetylene or by segregation of a carbon-doped crystal [49, 54, 55]. At the coverage $\Theta_C \approx \frac{1}{2}$, the adatoms form a c$(2\times 2)$ ordered arrangement residing in every second hollow site only $d_{01} = 0.46$ Å above the substrate. The substantial contraction of the first-layer spacing of the clean surface is reversed to a slight expansion (+3%). Also, the former depletion of Mo

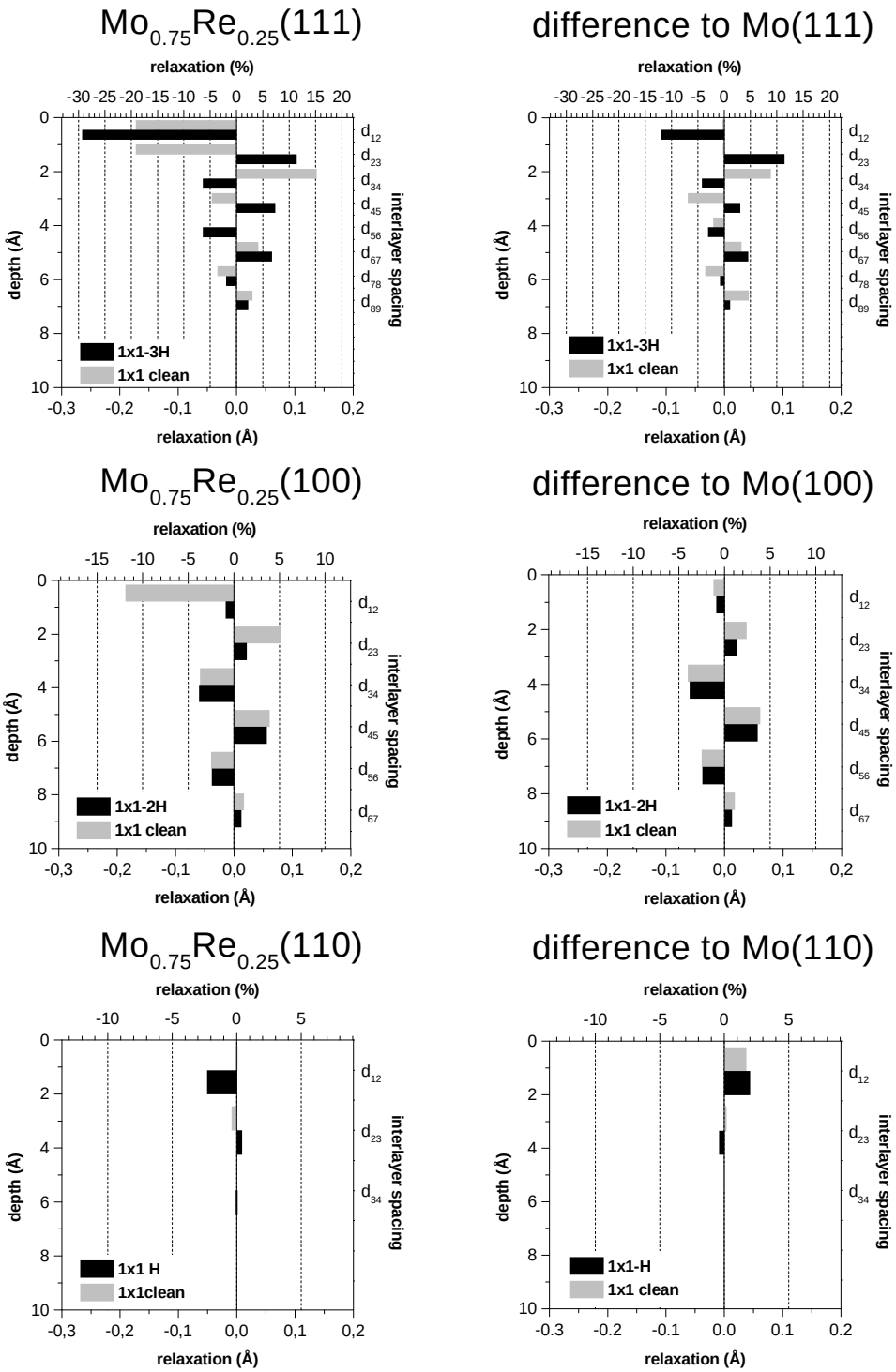

Figure 8. Bar diagrams for the multilayer relaxation of different clean and hydrogen-saturated $Mo_{75}Re_{25}$ surfaces (left-hand column). In the right-hand column the relaxational differences from the respective phases of clean Mo are given. The scales are kept the same in all graphs, so that the different layer spacings and relaxations for the different surface orientations become apparent.

in the second layer is largely removed, i.e. due to the strong Mo–C bonding additional Mo has segregated to the surface as expected. Accordingly, the concentration of Mo atoms below the c(2 × 2)-arranged C atoms is slightly higher than that for their neighbours accompanied by some atomic buckling in the second substrate layer. The carbon bond lengths to first- and second-layer Mo atoms (2.26 and 2.08 Å, respectively) are already near the value for cubic MoC (2.145 Å). This tendency to form MoC proceeds for coverages $\Theta_C \approx 1$ and $\Theta_C \approx 1.5$ for which 1×1 diffraction patterns are observed. With increasing amount of carbon in the surface, the top-substrate-layer spacing expands further ($\Delta d_{12}/d_0 \approx 15\%$ and 28%, respectively). This creates space for the accommodation of carbon atoms below the first layer, which indeed is detected already for $\Theta_C \approx 1.5$. At this coverage even the second-substrate-layer spacing has increased almost to the value of the first-layer spacing ($\Delta d_{23}/d_0 \approx 26\%$). The carbon atoms reside almost in the plane, i.e. within the much Mo-enriched first and second substrate layers, so forming a NaCl-type structure, as is characteristic for cubic MoC. The interlayer distance in ideal MoC is 2.15 Å, rather close to the values obtained, $d_{12} \approx d_{23} \approx 2.0$ Å. The 7.0% contraction in the vertical direction compares to a 5.8% expansion of the lateral unit mesh area enforced by the $Mo_{75}Re_{25}(100)$ substrate, i.e. we deal with a tetragonally distorted NaCl structure with the MoC unit-cell volume almost preserved.

For oxygen adsorption, the Mo–O binding energy being stronger than that for Re–O leads also to further Mo segregation in the $Mo_{75}Re_{25}(100)$ surface. With a full monolayer of oxygen adsorbed and upon annealing at temperatures at or above about 1400 K, the surface reconstructs heavily, exhibiting a 2×1 structure. Every second row of top-layer molybdenum atoms is removed (*missing-row reconstruction*) as found both by LEIS [56] and LEED investigations [53]. The adatoms reside $d_{01} = 0.32$ Å above the substrate at threefold-coordinated sites, i.e. they are bound to two top-layer atoms and to one atom of the second substrate layer (figure 9). These substrate bonding partners are nearly exclusively Mo atoms, as the 100% Mo concentration in the top layer remains and the second-layer Mo concentration increases from about 50 to 90%. Simultaneously, the first-substrate-layer spacing expands considerably ($\Delta d_{12}/d_0 = +7.7\%$ versus -11.6% for the clean surface) and the second-layer spacing contracts ($\Delta d_{23}/d_0 = -3.2\%$ versus +4.7%). This rearrangement is such that almost equal Mo–O bond lengths result (2.02–2.04 Å), equivalent to oxygen hard-sphere radii of 0.66–0.68 Å, which are typical for oxygen in tetrahedral covalent bonding surroundings.

4. Conclusions

The examples presented in this paper show that ideal stoichiometric terminations of bcc-type alloy surfaces corresponding to the bulk concentration are rather limiting cases. On the one hand, ordered alloys tend to develop some chemical disorder, whose extent seems to depend on the magnitude of the heat of formation of the alloy. Large values of this quantity favour the ordered, bulk-like termination; the lower the value, the greater the extent of segregation-induced chemical disorder in the first few surface layers. Even displacive surface reconstructions may take place to match to the modified surface stoichiometry. Additionally, a completely new kind of chemical order can also develop, in particular when as a result of the surface preparation procedures—e.g. (preferential) sputtering—the composition of the near-surface slab has been changed. On its way back to equilibrium during the annealing, the surface can run through new states of chemical order. Yet, though being practically stable at room temperature, such states in the thermodynamic sense may correspond to only local minima of the free energy, i.e. to metastable rather than stable phases. On the other hand, substitutionally disordered alloys are not expected to maintain the bulk stoichiometry in their surface layers. Again, the constituent with the lower homogeneous binding energy segregates to the top surface layer, so

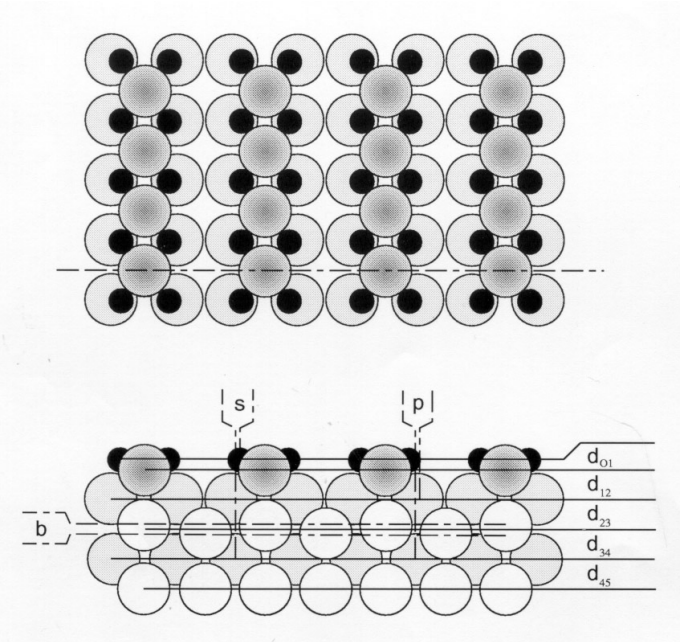

Figure 9. Top and side views (along the dashed line) of the oxygen-induced 2×1 missing-row reconstruction of the $Mo_{75}Re_{25}(100)$ surface (after reference [54]). The quantities b (=0.08 Å) and p (=0.04 Å) denote the second substrate layer's vertical buckling and lateral row-pairing amplitude, respectively. The quantity s (=0.29 Å) denotes the lateral displacement of the oxygen atom away from the second-layer top site.

simultaneously reducing the surface stress. With the heat of formation being slightly negative, this segregation at the actual surface leads to some depletion in the second layer, so initiating an oscillating concentration profile decaying with increasing surface depth. So, despite the ideal disorder in the bulk, some chemical order is established in a certain surface slab. This can be considerably modified by adsorbates.

This scenario certainly does not hold exclusively for bcc-type binary alloys. Yet, as regards geometrical modifications in the surface, bcc-type structures can exhibit rather large relaxations of layer spacings, so offering the chance to detect possible correlations between surface geometry and stoichiometry. Such correlations do indeed seem to exist, as deduced from the fact that—at least for the examples investigated so far—multilayer relaxations in alloy surfaces extend much deeper into the surface than those in the related pure-metal surfaces. It appears that the segregational profile stabilizes the relaxational profile, as is evident from the relaxational behaviour upon hydrogen adsorption on the alloy surface. Whilst the relaxations of the first few layer spacings are modified to practically the same extent as is detected for the pure metal, spacings deeper in the surface remain unaffected, as the influence of hydrogen has died away and that of the oscillating stoichiometry dominates. Certainly these features demand quantitative interpretation by means of first-principles calculations.

Acknowledgment

The authors are indebted to the Deutsche Forschungsgemeinschaft (DFG) for many years of financial support.

References

[1] Gauthier Y and Baudoing R 1990 *Segregation and Related Phenomena* ed P Dowben and A Miller (Boca Raton, FL: Chemical Rubber Company Press) p 169ff
[2] Bardi U 1994 *Rep. Prog. Phys.* **57** 939
[3] Krimmel S, Donner W, Nickel B, Dosch H, Sutter C and Grübel G 1997 *Phys. Rev. Lett.* **78** 3880
[4] Leidl R and Diehl H W 1998 *Phys. Rev.* B **57** 1908
[5] Rodriguez J A 1996 *Surf. Sci. Rep.* **24** 223
[6] Heinz K and Hammer L 1998 *Z. Kristallogr.* **213** 615
[7] Mullins D R and Overbury S H 1988 *Surf. Sci.* **199** 141
[8] Davis H L and Noonan J R 1985 *Phys. Rev. Lett.* **54** 566
[9] Davis H L and Noonan J R 1988 *The Structure of Surfaces II (Springer Series in Surface Sciences vol 11)* ed J F van der Veen and M A Van Hove (Berlin: Springer) p 152
[10] Yalisove S M and Graham W R 1987 *Surf. Sci.* **183** 556
[11] Kang M H and Mele E J 1987 *Phys. Rev.* B **36** 7371
[12] Lee J J, Fu C L and Freeman C L 1987 *Phys. Rev.* B **36** 931
[13] Hanbicki A, Baddorf A P, Plummer E W, Hammer B and Scheffler M 1995 *Surf. Sci.* **331–333** 811
[14] Blum V, Rath C, Castro G R, Kottcke M, Hammer L and Heinz K 1996 *Surf. Rev. Lett.* **3** 1409
[15] Kim S K, Tian Y, Jona F and Marcus P M 1997 *Phys. Rev.* B **56** 9858
[16] Hultgren R, Desai P D, Hawkins D T, Gleiser M and Kelley K K 1973 *Selected Values of the Thermodynamic Properties of Binary Alloys* (Metals Park, OH: American Society of Metals)
[17] Graupner H, Hammer L, Müller K and Zehner D M 1995 *Surf. Sci.* **322** 103
[18] Hammer L, Graupner H, Blum V, Heinz K, Ownby G W and Zehner D M 1998 *Surf. Sci.* **412+413** 69
[19] Davis H L and Noonan J R 1987 *Mater. Res. Soc. Symp. Proc.* **83** 3
[20] Wang C P, Jona F, Gleason N R, Strongin D R and Marcus P M 1993 *Surf. Sci.* **298** 114
[21] Blum R-P, Ahlenbehrendt D and Niehus H 1996 *Surf. Sci.* **366** 107
[22] Kottcke M, Graupner H, Zehner D M, Hammer L and Heinz K 1996 *Phys. Rev.* B **54** R5275
[23] Baddorf A P and Chandavarkar S S 1996 *Physica* B **221** 141
[24] Graupner H 1995 *Thesis* Universität Erlangen–Nürnberg
[25] Madey T E, Guan J, Nien C-H, Dong C-Z, Tao H-S and Campbell R A 1996 *Surf. Rev. Lett.* **3** 1315
[26] Williams F L and Nason D 1974 *Surf. Sci.* **45** 377
[27] Gray D E (ed) 1972 *American Institute of Physics Handbook* (New York: McGraw-Hill)
[28] Meier W, Hammer L and Heinz K 1999 unpublished
[29] Zehner D M 1996 *Surf. Rev. Lett.* **3** 1637
[30] Gaßmann P, Franchy R and Ibach H 1994 *Surf. Sci.* **319** 95
[31] Dannohl H D and Lukas H L 1974 *Z. Metallk.* **64** 642
[32] Henig E T and Lukas H L 1975 *Z. Metallk.* **66** 98
[33] Meschel S V and Kleppa O J 1994 *Metallic Alloys: Experimental and Theoretical Perspectives* ed R G Jordan (Dordrecht: Kluwer)
[34] Felter T E, Barker R A and Estrup P J 1977 *Phys. Rev. Lett.* **38** 1138
[35] Davis H L, Zehner D M, Dötsch B, Wimmer A and Müller K 1991 *Bull. Am. Phys. Soc.* **36** 705
[36] Döll R, Kottcke M, Heinz K, Hammer L, Müller K and Zehner D M 1994 *Surf. Sci.* **307–309** 434
[37] Kottcke M, Dötsch B, Hammer L, Heinz K, Müller K and Zehner D M 1997 *Surf. Sci.* **376** 319
[38] Wang X M, Chan C T and Ho K M 1987 *Phys. Rev. Lett.* **60** 2066
[39] Pendry J B 1980 *J. Phys. C: Solid State Phys.* **13** 937
[40] Overbury S H, van den Oetelaar R J A and Zehner D M 1993 *Phys. Rev.* B **48** 1718
[41] Lyman P F and Zehner D M 1994 *Metallic Alloys: Experimental and Theoretical Perspectives* ed J S Faulkner and R G Jordan (Dordrecht: Kluwer) p 113
[42] Jona F and Marcus P M 1988 *The Structure of Surfaces II (Springer Series in Surface Sciences vol 11)* ed J F van der Veen and M A Van Hove (Berlin: Springer) p 90
[43] Sokolov J, Jona F and Marcus P M 1986 *Phys. Rev.* B **33** 1397
[44] Hammer L, Kottcke M, Taubmann M, Meyer S, Rath C and Heinz K 1999 *Surf. Sci.* at press
[45] Arnold M, Sologub S, Hupfauer G, Bayer P, Frie W, Hammer L and Heinz K 1997 *Surf. Rev. Lett.* **4** 1291
[46] Arnold M, Fahmi A, Frie W, Hammer L and Heinz K 1999 *J. Phys.: Condens. Matter* **11** 1873
[47] Heinz K and Hammer L 1996 *Z. Phys. Chem.* **197** 173
[48] Heinz K and Hammer L 1997 *Phys. Status Solidi* a **159** 225
[49] Kottcke M 1997 *PhD Thesis* Universität Erlangen–Nürnberg
[50] Hammer L, Kottcke M, Weiß W, Wimmer A, Zehner D M and Heinz K 1998 *Surf. Sci.* **401** 455

[51] Hammer L, Kottcke M, Blum V, Wimmer A, Taubmann M, Meyer S, Rath C and Heinz K 1999 in preparation
[52] Hildner M L, Daley R S, Felter T E and Estrup T E 1991 *J. Vac. Sci. Technol.* A **9** 1604
[53] Hammer L, Seiferlein F, Dingfelder U, Kottcke M, Döll R, Heinz K and Müller K 1995 *Surf. Sci.* **337** 224
[54] Hammer L, Kottcke M, Heinz K, Müller K and Zehner D M 1996 *Surf. Rev. Lett.* **5+6** 1701
[55] Kottcke M, Döll R, Weiß W, Seiferlein F, Arabzyk W, Hammer L and Heinz K 1996 *Surf. Sci.* **352–354** 592
[56] Overbury S H and van den Oetelaar R J A 1994 *Surf. Sci.* **301** 313